Electronic Supplementary Material (ESI) for Physical Chemistry Chemical Physics.

Supporting Information

Doping of the Mn vacancy of Mn_2B_2 with a single different transition metal atom as the dual-function electrocatalyst

Jing Xu[a], Yusheng Wang[*a,c], Nahong Song[b,c], Shijun Luo[a], Bin Xu[a], Jing Zhang[a], Fei Wang[c]

[a] *College of Physics and Electronics, North China University of Water Resources and Electric Power, Zhengzhou, Henan, 450046, China*

[b] *College of Computer and Information Engineering, Henan University of Economics and Law, Zhengzhou, Henan, 450000, China*

[c] *International Laboratory for Quantum Functional Materials of Henan, School of Physics, Zhengzhou University, Zhengzhou 450001, China*

Corresponding author: wangyusheng@ncwu.edu.cn

Figures

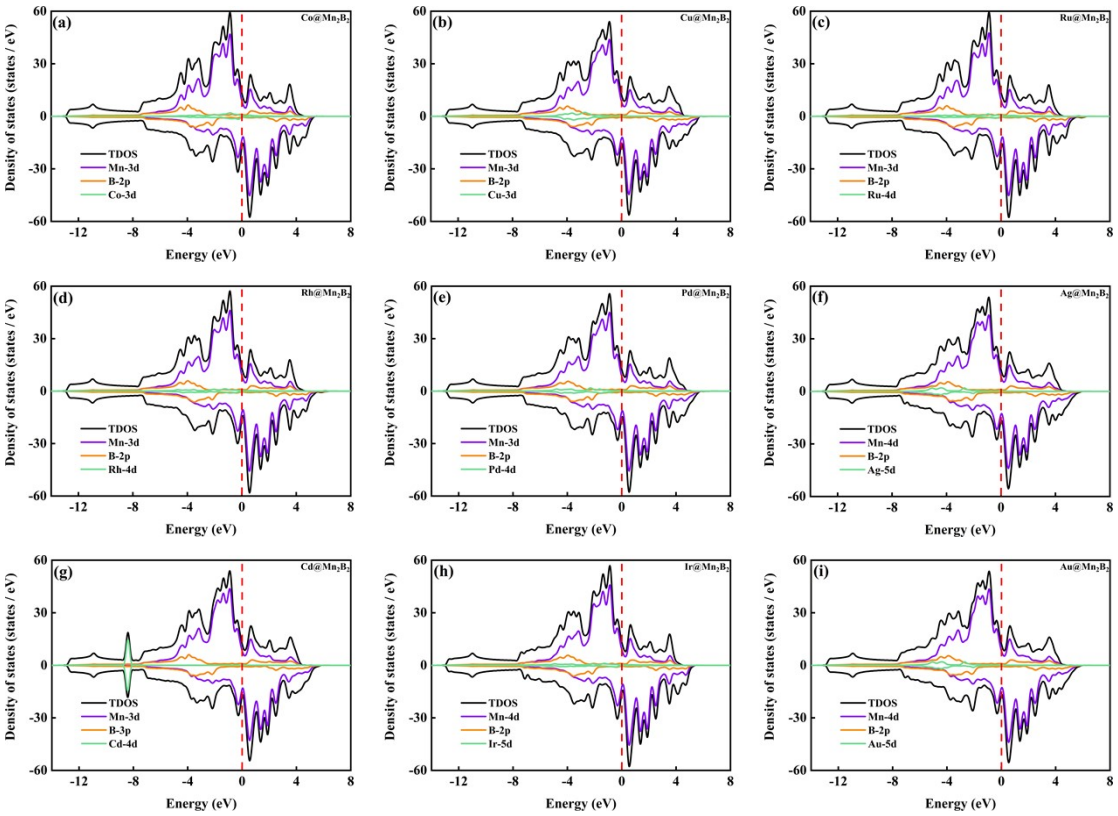

Fig. S1 The total density of states (TDOS) and projected density of states (PDOS) for (a) $Co@Mn_2B_2$, (b) $Cu@Mn_2B_2$, (c) $Ru@Mn_2B_2$, (d) $Rht@Mn_2B_2$, (e) $Pd@Mn_2B_2$, (f) $Ag@Mn_2B_2$, (g) $Cd@Mn_2B_2$, (h) $Ir@Mn_2B_2$ and (i) $Au@Mn_2B_2$, where the Fermi level was set to 0 eV.

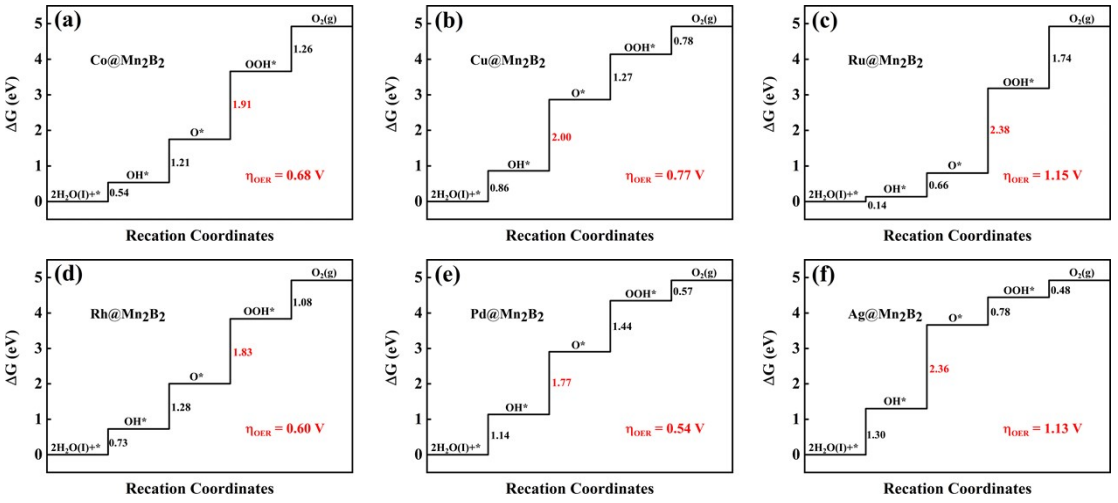

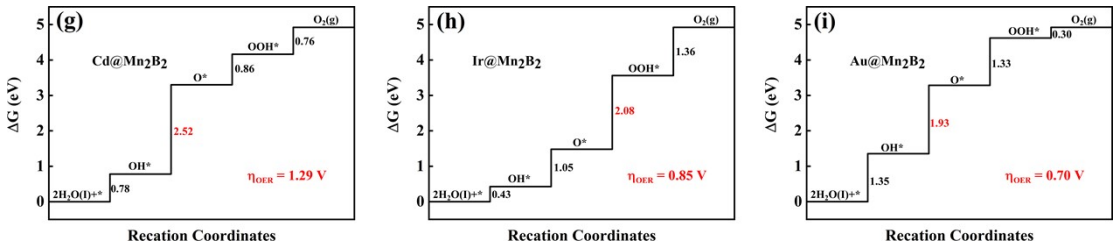

Fig. S2 The Gibbs free energy diagrams for the OER pathway of (a) Co@Mn_2B_2, (b) Cu@Mn_2B_2, (c) Ru@Mn_2B_2, (d) Rh@Mn_2B_2, (e) Pd@Mn_2B_2, (f) Ag@Mn_2B_2, (g) Cd@Mn_2B_2, (h) Ir@Mn_2B_2 and (i) Au@Mn_2B_2 at an electrode potential of 0 V.

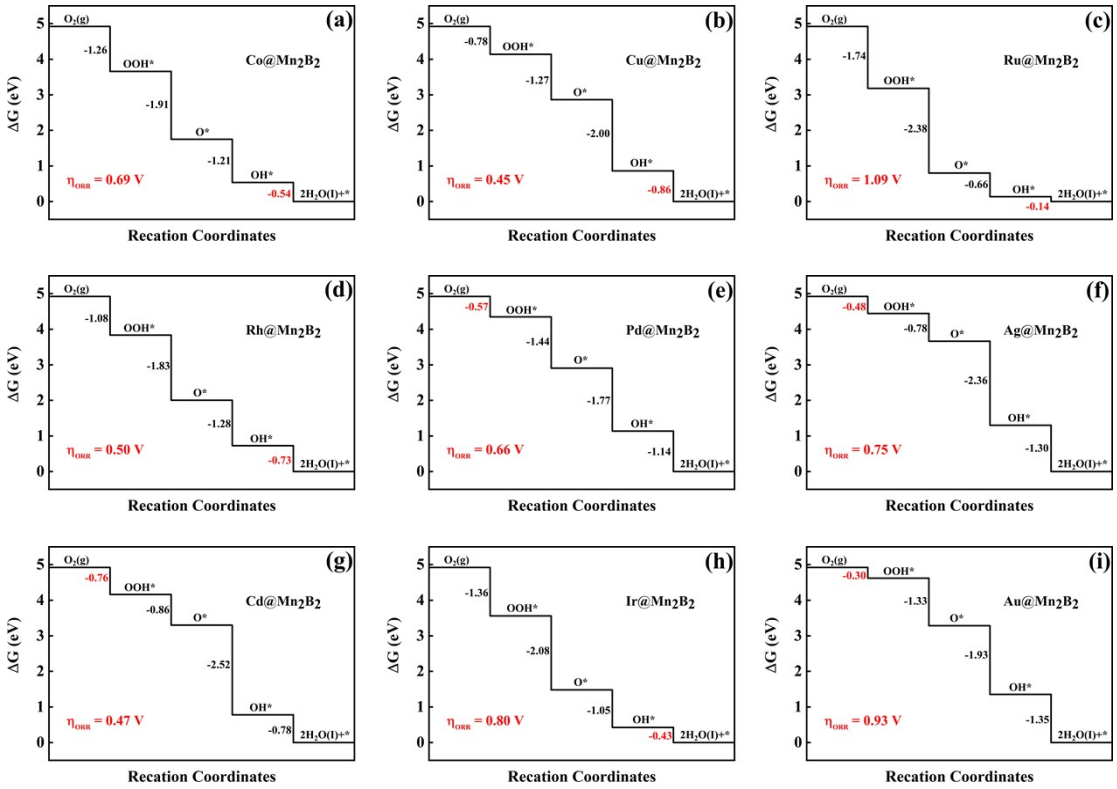

Fig. S3 The Gibbs free energy diagrams for the ORR pathway of (a) Co@Mn_2B_2, (b) Cu@Mn_2B_2, (c) Ru@Mn_2B_2, (d) Rh@Mn_2B_2, (e) Pd@Mn_2B_2, (f) Ag@Mn_2B_2, (g) Cd@Mn_2B_2, (h) Ir@Mn_2B_2 and (i) Au@Mn_2B_2 at an electrode potential of 0 V.

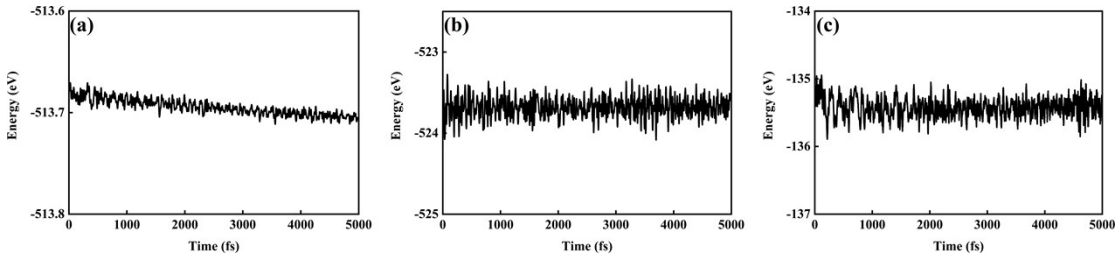

Fig. S4 The evolution trends of the total energy of (a) a 4×4 supercell with an -OH adsorbed, (b) a 4×4 supercell with two -OH adsorbed and (c) a 2×2 supercell with an -OH adsorbed.

Tables

Table S1 The binding energy E_b (eV) of a single different transition metal atoms embedded in the Mn vacancies of Mn_2B_2.

TM	E_b/eV
Co	-7.97
Ni	-7.00
Cu	-4.59
Ru	-10.10
Rh	-8.11
Pd	-5.33
Ag	-3.36
Cd	-1.85
Ir	-10.24
Pt	-7.81
Au	-4.17

Table S2 The binding free energy (ΔG_1, ΔG_2, ΔG_3 and ΔG_4) and theoretical overpotential (η_{OER}) of the OER for different transition metal atoms.

TM@Mn_2B_2	ΔG_1/eV	ΔG_2/eV	ΔG_3/eV	ΔG_4/eV	η_{OER}/V
Co@Mn_2B_2	0.54	1.21	1.91	1.26	0.68
Ni@Mn_2B_2	0.86	1.53	1.61	0.91	0.38
Cu@Mn_2B_2	0.86	2.00	1.27	0.78	0.77
Ru@Mn_2B_2	0.14	0.66	2.38	1.74	1.15
Rh@Mn_2B_2	0.73	1.28	1.83	1.08	0.60
Pd@Mn_2B_2	1.14	1.77	1.44	0.57	0.54
Ag@Mn_2B_2	1.30	2.36	0.78	0.48	1.13
Cd@Mn_2B_2	0.78	2.52	0.86	0.76	1.29
Ir@Mn_2B_2	0.43	1.05	2.08	1.36	0.85
Pt@Mn_2B_2	1.00	1.52	1.68	0.71	0.45
Au@Mn_2B_2	1.35	1.93	1.33	0.30	0.70

Table S3 The binding free energy (ΔG_a, ΔG_b, ΔG_c and ΔG_d) and theoretical overpotential (η_{ORR}) of the ORR for different transition metal atoms.

TM@Mn_2B_2	ΔG_a/eV	ΔG_b/eV	ΔG_c/eV	ΔG_d/eV	η_{ORR}/V
Co@Mn_2B_2	-1.26	-1.91	-1.21	-0.54	0.69
Ni@Mn_2B_2	-0.91	-1.61	-1.53	-0.86	0.37
Cu@Mn_2B_2	-0.78	-1.27	-2.00	-0.86	0.45
Ru@Mn_2B_2	-1.74	-2.38	-0.66	-0.14	1.09
Rh@Mn_2B_2	-1.08	-1.83	-1.28	-0.73	0.50
Pd@Mn_2B_2	-0.57	-1.44	-1.77	-1.14	0.66
Ag@Mn_2B_2	-0.48	-0.78	-2.36	-1.30	0.75
Cd@Mn_2B_2	-0.76	-0.86	-2.52	-0.78	0.47
Ir@Mn_2B_2	-1.36	-2.08	-1.05	-0.43	0.80
Pt@Mn_2B_2	-0.71	-1.68	-1.52	-1.00	0.52
Au@Mn_2B_2	-0.30	-1.33	-1.93	-1.35	0.93

Table S4 The adsorption energy *E*a (eV) of OH^*, O^*, OOH^* and H^* for different doped transition metal atoms.

TM@Mn_2B_2	*E*a(OH^*)/eV	*E*a(O^*)/eV	*E*a(OOH^*)/eV	*E*a(H^*)/eV
Co@Mn_2B_2	-3.45	-5.59	-2.18	-3.56
Ni@Mn_2B_2	-3.13	-4.95	-1.78	-3.22
Cu@Mn_2B_2	-3.09	-4.45	-1.69	-2.92
Ru@Mn_2B_2	-3.84	-6.55	-2.58	-3.83
Rh@Mn_2B_2	-3.27	-5.34	-1.98	-3.59
Pd@Mn_2B_2	-2.81	-4.40	-1.45	-3.19
Ag@Mn_2B_2	-2.68	-3.66	-1.38	-2.72
Cd@Mn_2B_2	-3.18	-4.03	-1.64	-2.90
Ir@Mn_2B_2	-3.54	-5.87	-2.24	-4.07
Pt@Mn_2B_2	-2.98	-4.81	-1.59	-3.70
Au@Mn_2B_2	-2.64	-4.05	-1.20	-3.26

Table S5 The *d*-band centers (ε_d) of TM@Mn_2B_2.

TM@Mn_2B_2	ε_d (eV)
Co@Mn_2B_2	-1.40
Ni@Mn_2B_2	-1.82
Cu@Mn_2B_2	-3.01
Ru@Mn_2B_2	-1.81
Rh@Mn_2B_2	-2.23
Pd@Mn_2B_2	-2.80
Ag@Mn_2B_2	-3.93
Cd@Mn_2B_2	-8.20
Ir@Mn_2B_2	-2.74
Pt@Mn_2B_2	-3.37
Au@Mn_2B_2	-3.77

Table S6 The binding free energy ΔG_H (eV) of the HER for different transition metal atoms.

TM@Mn_2B_2	ΔG_H/eV
Co@Mn_2B_2	-0.05
Ni@Mn_2B_2	0.25
Cu@Mn_2B_2	0.56
Ru@Mn_2B_2	-0.32
Rh@Mn_2B_2	-0.08
Pd@Mn_2B_2	0.31
Ag@Mn_2B_2	0.75
Cd@Mn_2B_2	0.57
Ir@Mn_2B_2	-0.53
Pt@Mn_2B_2	-0.16
Au@Mn_2B_2	0.24

Table S7 The binding free energy (ΔG_1, ΔG_2, ΔG_3 and ΔG_4) and theoretical overpotential (η_{OER}) of the OER for a single Mn atom of Mn_2B_2.

	ΔG_1/eV	ΔG_2/eV	ΔG_3/eV	ΔG_4/eV	η_{OER}/V
Mn_2B_2	-0.21	0.49	2.58	2.06	1.35

Table S8 The binding free energy (ΔG_a, ΔG_b, ΔG_c and ΔG_d) and theoretical overpotential (η_{ORR}) of the ORR for a single Mn atom of Mn_2B_2.

	ΔG_a/eV	ΔG_b/eV	ΔG_c/eV	ΔG_d/eV	η_{ORR}/V
Mn_2B_2	-2.06	-2.58	-0.49	0.21	1.44

Table S9 The adsorption energy *E*a (eV) of OH^*, O^*, OOH^* and H^* for a single Mn atom of Mn_2B_2.

	*E*a(OH^*)/eV	*E*a(O^*)/eV	*E*a(OOH^*)/eV	*E*a(H^*)/eV
Mn_2B_2	-4.17	-7.07	-2.96	-3.47

Table S10 The binding free energy ($\Delta G_1/\Delta G_a$, $\Delta G_2/\Delta G_b$, $\Delta G_3/\Delta G_c$ and $\Delta G_4/\Delta G_d$) and theoretical overpotential (η_{OER}/η_{ORR}) of the Ni@Mn_2B_2 without DFT-D2 vdw correction.

TM@Mn_2B_2	$\Delta G_1/\Delta G_a$	$\Delta G_2/\Delta G_b$	$\Delta G_3/\Delta G_c$	$\Delta G_4/\Delta G_d$	η_{OER}/η_{ORR}
Ni@Mn_2B_2	1.04/-0.87	1.40/-1.61	1.61/-1.40	0.87/-1.04	0.38/0.36

Table S11 The binding energy E_b (eV), theoretical overpotential (η_{OER}) of the OER, theoretical overpotential (η_{ORR}) of the ORR and the binding free energy ΔG_H (eV) of the HER.

TM@Mn_2B_2	E_b/eV	η_{OER}/V	η_{ORR}/V	ΔG_H/eV
Ir	-10.24	0.85	0.8	-0.53
Ru	-10.1	1.15	1.09	-0.32
Rh	-8.11	0.6	0.5	-0.08
Co	-7.97	0.68	0.69	-0.05
Pt	-7.81	0.45	0.52	-0.16
Ni	-7	0.38	0.37	0.25
Pd	-5.33	0.54	0.66	0.31
Cu	-4.59	0.77	0.45	0.56
Au	-4.17	0.7	0.93	0.24
Ag	-3.36	1.13	0.75	0.75
Cd	-1.85	1.29	0.47	0.57

Hydrogen coverage:

we used fifteen Mn atoms generated from one surface of the 4×4 supercell and a single metal atom replacing Mn as the active site of the HER intermediate H^+ (total sixteen adsorption sites). For example, 1/4 of the coverage stated in the manuscript is four H^+ adsorbed at four different sites. The number of adsorption structures formed due to the arrangement and combination of fifteen Mn atoms with a single metal atom are high, so we selected the other three positions closest to the single metal atom. The results for the 1/4 hydrogen coverage are still calculated based on the 1/16 hydrogen coverage calculation method, except that one H^+ is replaced by four H^+.